Published in final edited form as:
Dev Cell. 2010 May 18; 18(5): 750–762. doi:10.1016/j.devcel.2010.03.009.

Phosphatase-dependent and -independent Functions of Shp2 in Neural Crest Cells Underlie LEOPARD Syndrome Pathogenesis

Rodney A. Stewart[1,2,*], **Takaomi Sanda**[1,9], **Hans R. Widlund**[3,9], **Shizhen Zhu**[1], **Kenneth D. Swanson**[4], **Aeron D. Hurley**[1,3], **Mohamed Bentires-Alj**[4,5], **David E. Fisher**[1,6], **Maria I. Kontaridis**[4,7], **A. Thomas Look**[1,*], and **Benjamin G. Neel**[4,8,*]

[1]Dana-Farber Cancer Institute, Dept. of Pediatric Oncology, Harvard Medical School, Boston, MA 02115

[2]Huntsman Cancer Institute, Dept. of Oncological Sciences, University of Utah, Salt Lake City, UT 84112

[3]Brigham and Women's Hospital, Dept. of Dermatology, Harvard Medical School, Boston, MA 02115, USA

[4]Beth Israel Deaconess Medical Center, Cancer Biology Program, Boston, MA 02115

SUMMARY

The tyrosine phosphatase SHP2 (*PTPN11*) regulates cellular proliferation, survival, migration and differentiation during development. Germline mutations in *PTPN11* cause Noonan and LEOPARD syndromes, which have overlapping clinical features. Paradoxically, Noonan syndrome mutations increase SHP2 phosphatase activity, while LEOPARD syndrome mutants are catalytically impaired, raising the possibility that SHP2 has phosphatase-independent roles. By comparing *shp2*-deficient zebrafish embryos with those injected with mRNA encoding LEOPARD syndrome point mutations, we identify a phosphatase- and Erk-dependent role for Shp2 in neural crest specification and migration. We also identify an unexpected phosphatase-and Erk-independent function, mediated through its SH2 domains, which is evolutionarily conserved and prevents p53-mediated apoptosis in the brain and neural crest. Our results indicate that previously enigmatic aspects of LEOPARD syndrome pathogenesis can be explained by the combined effects of loss of Shp2 catalytic function and retention of an SH2 domain-mediated role that is essential for neural crest cell survival.

INTRODUCTION

The non-receptor tyrosine phosphatase SHP2 (*PTPN11*) plays a key role in signaling by receptor tyrosine kinases (RTKs), cytokine receptors and integrins (Feng, 1999; Neel et al., 2009). A ubiquitously expressed molecule with two N-terminal SH2 domains, a catalytic

[*] To whom correspondence should be addressed.
[5]Current Address, Friedrich Miescher Institute for Biomedical Research, Basel, Switzerland
[6]Current Address, Massachusetts General Hospital, Dept. of Dermatology, Charlestown, Harvard Medical School, MA 02129
[7]Current Address, Beth Israel Deaconess Medical Center, Dept. of Cardiology, Harvard Medical School, Boston, MA 02115, USA
[8]Current Address, Ontario Cancer Institute, Toronto Medical Discovery Tower, Ontario M5G 1L7
[9]Equal contribution

(PTP) domain, and a C-terminus with tyrosyl phosphorylation sites and a prolyl-rich stretch, SHP2 is regulated via an elegant mechanism that couples intracellular localization to catalytic activation (Barford and Neel, 1998; Hof et al., 1998). In the absence of cell stimulation, SHP2 exists in an inactive, “closed” conformation with its N-terminal SH2 domain (N-SH2) wedged into the catalytic cleft, blocking substrate access. Upon receptor activation, SHP2 is recruited via its SH2 domains to specific cellular phosphotyrosyl (pTyr) proteins, which include some RTKs themselves, scaffolding adapters, or immune inhibitory receptors (Feng, 1999; Neel et al., 2009). Binding of an appropriate pTyr-protein to the N-SH2 domain of SHP2 abrogates inhibition of the PTP domain, resulting in an “open” structure and phosphatase activation.

Although its key substrates remain controversial, much evidence has established that appropriate localization of SHP2 and its catalytic activity are required for full activation of the RAS/ERK cascade (Neel et al., 2009). In tissue culture cells, catalytically inactive SHP2 mutants have dominant negative effects on multiple RTK and integrin signaling pathways, inhibiting RAS/ERK activation, cell proliferation, focal adhesion turnover and cell spreading and migration (Neel et al., 2009). Mutations in the *Drosophila* SHP2 ortholog *corkscrew* also impair RTK signaling, and are rescued by gain-of-function mutants in Ras/Erk cascade components (Allard et al., 1996; Perkins et al., 1992). Dominant negative SHP2 blocks fibroblast growth factor-evoked Erk activation, mesodermal gene induction and gastrulation in *Xenopus* (O'Reilly and Neel, 1998; Tang et al., 1995). Gastrulation is also defective in mouse embryos homozygous for a hypomorphic *Ptpn11* mutation, and cells from these embryos show impaired Ras/Erk activation in response to multiple stimuli (Saxton et al., 1997; Shi et al., 2000; Zhang et al., 2004). In contrast, homozygous null *Ptpn11* mutation leads to peri-implantation lethality due, at least in part, to defective Erk activation and trophoblast stem cell death via a Bim-dependent pathway (Yang et al., 2006). SHP2 has cell type- and receptor-specific roles in PI3K, Rho, NFκB and NFAT activation, but in those cases analyzed carefully, SHP2 catalytic activity also appears to be required (Neel et al., 2009).

Improper regulation of SHP2 can lead to disease. Germline *PTPN11* mutations cause ~50% of Noonan syndrome (NS) cases and the vast majority of LEOPARD syndrome (LS) cases (Tartaglia and Gelb, 2005). NS displays some combination of cardiac (most often valvuloseptal) abnormalities, proportional short stature, and facial dysmorphia (e.g., ocular hypertelorism) and a variety of less penetrant defects (e.g., cognitive, genitourinary, auditory abnormalities). LEOPARD is an acronym for multiple lentigines, electrocardiographic abnormalities, ocular hypertelorism, pulmonary stenosis, abnormal genitalia, retardation of growth, and sensorineural deafness. Somatic *PTPN11* mutations are the most common cause of juvenile myelomonocytic leukemia, and occur more rarely in solid tumors (Mohi and Neel, 2007).

Because LS and NS share several features, they are generally viewed as overlapping syndromes. Other evidence suggests that their pathogenesis is distinct. Lentigines (dark frecklelike lesions containing melanocytes) are characteristic of LS, but not NS (Tartaglia and Gelb, 2005). Hypertrophic cardiomyopathy is common in LS, yet rare in *PTPN11*-associated NS (Digilio et al., 2006; Ogata and Yoshida, 2005). NS patients often show transient myeloproliferation and rarely develop juvenile myelomonocytic leukemia (Bader-Meunier et al., 1997). LS patients may be predisposed to other malignancies, such as acute leukemia and neuroblastoma (Merks et al., 2005; Ucar et al., 2006).

Most importantly, the biochemical properties of disease-associated PTPN11 proteins are distinct. Nearly all *PTPN11* mutations identified in NS and human tumors affect residues at the interface between the N-SH2 and PTP domains, resulting in enhanced SHP2 catalytic

activity and RAS/ERK activation in vitro (Fragale et al., 2004; Keilhack et al., 2005; Niihori et al., 2005; Tartaglia et al., 2006) and in vivo (Araki et al., 2004). Gain-of-function alleles of *KRAS* (Schubbert et al., 2006), *SOS1* (Roberts et al., 2007; Tartaglia et al., 2007) or *RAF1* (Pandit et al., 2007; Razzaque et al., 2007) also cause NS, providing genetic evidence that this syndrome results from inappropriately high RAS/ERK pathway activity. In contrast, LS mutations target the PTP domain, typically involve catalytic residues, and result in variants with substantially decreased/absent phosphatase activity that act as dominant negative mutants in transfection assays (Hanna et al., 2006; Kontaridis et al., 2006; Tartaglia et al., 2006). These findings pose two related questions: How do syndromes with overlapping features result from mutations with opposite effects on the catalytic activity and, apparently, the biological function of SHP2? And are LS mutations pure dominant negative alleles or do they also have phosphatase-independent activities that mediate LS phenotypes?

Many LS features (e.g., altered pigmentation, craniofacial defects, semilunar valve disorders) could involve defects in the neural crest. Zebrafish provide an excellent system for studying neural crest development because of their transparency and highly conserved molecular pathways. Therefore, we compared the effects of antisense morpholinos (*shp2* MO) and LS mutant mRNAs on zebrafish neural crest development.

RESULTS

LS Mutations Have Dominant Negative Effects on Zebrafish Gastrulation

Zebrafish Shp2 is highly similar (92% identical) to its mammalian orthologs and is expressed ubiquitously during gastrulation (Figures S1A–B; Jopling et al., 2007). If LS mutants only have dominant negative effects on development, then these should be qualitatively similar to the effects caused by Shp2 deficiency. We compared zebrafish embryos injected with mRNAs for LS mutants (engineered into zebrafish *shp2*) with those injected with *shp2* MOs to block Shp2 expression (Figure 1A). This experiment tested three LS alleles (Y280C, A462T and T469M, corresponding to the human LS alleles Y279C, A461T and T468M, Figure S1A), as well as two *shp2* MOs that block either translation or splicing (Figures S1C–D). As reported earlier (Jopling et al., 2007), LS (A462T) mRNA or *shp2* MO injections caused similar gastrulation defects, which were rescued by co-expression of wild-type (WT) human *SHP2* (Figures 1A, S1E). Both MOs, but not a control "mismatch" MO (mmMO), depleted Shp2 and impaired Erk activation (Figure 1B). Increasing amounts of *shp2* LS mRNA caused a dose-dependent decrease in Erk activation (Figure 1C). In contrast, over-expressing WT zebrafish (or human) *shp2* did not affect Erk activity or development (Figures 1A, B; see Experimental Procedures). Thus, LS mutants and *shp2* deficiency have similar effects on phospho-Erk levels and early embryonic events, consistent with LS mutations acting as dominant negative alleles.

Neomorphic Effects of LS Mutants on Neural Crest Development

We next compared the effects of LS mRNAs or *shp2* MOs on neural crest development. At 6 days post-fertilization (dpf), >90% of embryos injected with *shp2* MOs had markedly abnormal craniofacial skeletons, including incomplete fusion and posterior displacement of the first and second arch and loss of the third to seventh branchial arches (Figure 1D; middle panels). LS mRNAs caused craniofacial dysmorphia in ~50% of embryos, although these defects were milder, with arch elements preserved but reduced in size and the first and second arches posteriorly displaced (Figure 1D, bottom panels). The remaining LS embryos (50%) had severe gastrulation phenotypes that prevented analysis, mild 'hammerhead' phenotypes, as described previously (Jopling et al., 2007) or no obvious phenotype.

In contrast, the effects of *shp2* MOs and LS mRNA on pigment cell development were quite distinct (Figures 1E–G). At 2 dpf, morphants had significantly fewer pigment cells, with iridophores reduced by ~70% and melanophores by ~35% (Figures 1E and S1F). Conversely, LS mRNA-injected embryos with neural crest defects displayed an ~ 45% increase in iridophores and an ~ 20% increase in melanophores. The increase in melanophores was even more evident at 6 dpf (Figure 1F); indeed, the pigmentation phenotype of LS mRNA-injected embryos (increased melanophores) resembled multiple lentigines, a hallmark of LS and a major phenotypic difference between NS and LS (Figures 1E, F and S1F). Pigment cells from LS mRNA- and MO-injected embryos also showed delayed migration over the yolk towards the ventral stripe (Figure 1G, arrow).

Peripheral sympathetic nervous system development also differed in LS mRNA- and MO-injected embryos. There was an ~40% increase in tyrosine hydroxylase (*th*)-positive sympathetic neurons at 4 dpf in LS embryos, whereas morphants had an ~ 60% decrease in these cells (Figure S1G). Morphants, but not LS mRNA-injected embryos, also had abnormalities in their sensory cranial ganglia, dorsal root ganglia, and enteric neurons (Figures S1H, I). Other neural crest-derived tissues (e.g., neural crest-derived glia) were unaffected by either LS mRNA or *shp2* MO injections (data not shown), while *shp2* MO- and LS-injected embryos both displayed cardiac defects (Figure 1G, arrowhead), as described previously (Jopling et al., 2007).

Thus, although LS mutants and *shp2* deficiency have similar effects on gastrulation, LS mutants exert prominent neomorphic effects on neural crest development (distinct from those of *shp2* deficiency), suggesting that Shp2 has some function(s) independent of its PTP activity. Indeed, co-injection of LS mRNA and *shp2* MO caused neural crest phenotypes similar to those caused by LS mRNA injection alone, showing that LS molecules (which are catalytically impaired) restore some of the functions of Shp2 (Figure S1J).

Shp2- and Erk-dependent Requirement for Neural Crest Specification and Migration

Neural crest progenitors are induced at the neural plate border at approximately 10 hpf, and express transcription factors such as *foxd3*, *snai1b*, *tfap2α* and *sox10* (Kelsh and Raible, 2002; Stewart et al., 2006). These genes were induced properly in neural crest progenitors from MO- or LS mRNA-injected embryos (Figure S2A); however, marker expression in both LS- and *shp2* MO-injected embryos differed (from control embryos) at later times. At 16–18 somites, *sox10* mRNA levels in migrating cranial neural crest cells were higher in *shp2* morphants and, to a lesser extent, in LS mRNA-injected embryos (Figure 2A, arrows). The smaller effect of LS mRNA injection on *sox10* levels most likely reflects incomplete interference with Shp2 function and Erk activation (see below). At the same stage, *foxd3* expression in trunk neural crest cells (which give rise to pigment cells) was increased in MO- and LS mRNA-injected embryos (Figure 2A, arrowheads), and by 24 hpf, *sox10* levels were increased (Figure 2B, arrows). WT embryos treated with the MEK inhibitor U0126 at the tail-bud stage (post-gastrulation) also showed increased *sox10* and *foxd3* expression in cranial and trunk neural crest progenitors at the 14- and 17-somite stages respectively (Figure 2A). Thus, decreased Erk activity, as a consequence of impaired Shp2 catalytic function (rather than the indirect effects of impaired gastrulation), alters *sox10* and *foxd3* expression.

High *Sox10* expression maintains neural crest multipotency and inhibits differentiation (Kim et al., 2003; McKeown et al., 2005), whereas zebrafish *sox10* mutants show complete loss of pigment cells and other non-ectomesenchymal neural crest lineages (Dutton et al., 2001). Foxd3 also is linked to neural crest stem cell potentiality (Teng et al., 2008). To test the functional significance of the increased *sox10* and *foxd3* expression in *shp2* MO- and LS mRNA-injected embryos, we ectopically expressed these genes in WT embryos. Pigment

cell number was not altered by constitutive expression of *foxd3* mRNA (data not shown). But conditional expression of *sox10* (Arduini et al., 2009) at the 16- to 18-somite stage caused increased pigmentation (~20%) at 3 dpf, resembling the LS embryo phenotype (Figure 2C). Thus, at least one consequence of defective Shp2 activity and decreased Erk signaling during neural crest development, the up-regulation of *sox10*, clearly plays an important role in determining pigment cell number.

Neural crest migration also was abnormal in LS mRNA- or *shp2* MO-injected embryos. Normally, cranial neural crest cells migrate into ventral regions in the head by the 16 to 18-somite stage. However, in LS mRNA- or *shp2* MO-injected embryos, or in WT embryos treated with U0126, the *sox10*$^{+}$ cranial neural crest cells spread laterally over the head (Figure 2A, cranial view). Trunk neural crest cells normally show a gradient of migration, commencing with the most anterior neural crest cells (Figure 2B, control). The migration of *sox10*$^{+}$ trunk neural crest cells was markedly delayed in MO- and, to a lesser extent, in LS-injected embryos at 24 hpf (Figure 2B, arrowhead). Thus, Shp2 catalytic function and downstream Erk activation are required for specification of neural crest progenitors and their subsequent migration (also see Figure 7D).

Shp2 Deficiency Causes Apoptosis in the Brain and Neural Tube

Either LS mRNA- or MO-injection blocks neural crest progenitor differentiation and migration (Figure 2), yet their ultimate effects on neural crest-derived tissues differ dramatically (Figure 1). In an attempt to resolve this paradox, we examined later events in neural crest development. Expression of *crestin*, a pan-neural crest marker, appeared normal in LS-injected mutants at 24 hpf. In marked contrast, in morphants, *crestin* levels were reduced significantly in neural crest cells located posterior to the otic placode (Figure 3A, arrows). These cells generate multiple neural crest lineages that are severely reduced in *shp2*-deficient embryos. Expression of *dlx2*, which labels migrating branchial arch precursors, also was reduced or absent in *shp2* morphants (Figure 3B, arrows). An antibody specific for cleaved and activated Caspase-3 is a commonly used marker for apoptosis, and analysis of this marker from 10–36 hpf in WT (or LS mRNA-injected; see below) embryos showed minimal cell death. In contrast *shp2* MO-injected embryos were positive for cleaved Caspase-3, beginning at 18 hpf and persisting until 28 hpf (Figure 3C and data not shown). Increased cell death was observed in multiple tissues (e.g., the brain), but also was quite prominent in the neural tube region corresponding to the developing neural crest (compare arrows in Figures 3A–C). Double labeling with *crestin* and activated Caspase-3 confirmed that apoptosis was induced both in neural crest and surrounding neural tissue (data not shown).

To better define this cell death pathway, we surveyed the expression of upstream activators of Caspase-3 in zebrafish (Jette et al., 2008). At 18 hpf, the pro-apoptotic gene *puma* was widely expressed in *shp2* morphants, but not LS mRNA-injected (or WT) embryos, and became restricted to the brain and spinal cord at 24 hpf (Figure 3D, arrow). Morphants showed a marked increase in nuclei that labeled with the DNA damage-associated histone γ-H2Ax at 12 hpf (Figure 3E), suggesting that *shp2* deficiency induces DNA double-strand breaks in cells, resulting in a DNA damage-dependent apoptotic response. Blocking this pathway by injecting *shp2* MO into *p53* mutant embryos (to prevent *puma* induction), or co-injecting WT embryos with *shp2* MO and anti-apoptotic *bcl-2* or *bcl-xl* mRNA (to sequester excess Puma), completely rescued cell death, indicating that it is mediated by triggering the mitochondrial or intrinsic apoptotic pathway (Figure 3F and data not shown). Antisense morpholinos can cause developmental delay and toxic off-target effects, some of which are rescued by *p53* deficiency (Robu et al., 2007). But WT *SHP2* rescued the developmental and apoptotic effects of *shp2* knockdown, indicating that *shp2* specifically suppresses apoptosis in the neural tube (see Figure 4).

To determine the extent to which enhanced cell death accounts for the morphant phenotype (and hence the differences between MO- and LS mRNA-injected embryos), we examined later events in neural crest development in embryos co-injected with MO and *bcl-xl* mRNA (Figure 3G). As in LS mRNA-injected embryos, the number of pigment cells in MO/*bcl-xl*-co-injected embryos was increased compared with WT embryos, although their migration remained significantly delayed (white arrows in Figure 3G). Blocking cell death in morphants also restored *crestin* and *dlx* expression in migrating neural crest cells, normalized the number of *th*-positive sympathetic neurons, cranial sensory neurons and enteric neurons (data not shown), and ameliorated the craniofacial defects, as indicated by partial rescue of branchial arches 3–7, more complete fusion of the hyoid arch and an increase in the overall size of the head skeleton (Figure 3G, arrows).

These findings suggest that the main difference between the effects of LS mutants and Shp2 deficiency is that the latter causes apoptosis in the brain and neural tube. Because LS mutations impair PTP activity and ERK activation, the anti-apoptotic effect of Shp2 must be independent of its catalytic activity.

Shp2 Prevents Cell Death via a SH2 Domain-dependent Pathway

To gain further insight into how Shp2 prevents cell death, we co-injected *shp2* MO with mRNAs encoding Shp2 deletion or point mutants, all of which yielded stable Shp2 variants in embryos (Figures 4A, B, S1A and S3B). As noted above, co-expression of WT *shp2* mRNA rescued the excess cell death observed in *shp2* MO embryos (Figures 4B–E). Importantly, and consistent with the phenotype of WT embryos injected with LS mRNAs, coinjection of LS mRNA also rescued cell death (Figures 4B, F). As LS mutants have residual PTP activity (at least for some substrates), we tested the effect of a mutant in which an LS allele (A462T) was combined with the PTP-inactivating mutation R466M, which replaces the essential arginine in the catalytic pocket (Figures 4B, G). This construct, as well as a deletion mutant that removes the PTP-domain and the C-terminal tail of Shp2 (Figures 4B, H), also prevented cell death. In addition, treatment of WT embryos with U0126 blocked Erk activation (Figure S3A), but did not promote neural crest cell death (Figures 4B, I).

These results indicate that the PTP-independent, anti-apoptotic role of Shp2 is Erk-independent and mediated by the Shp2 N-terminus, which contains two SH2 domains. To address whether either or both SH2 domains must bind pTyr-peptides for the anti-apoptotic function of Shp2, we mutated the essential arginyl residue within the critical “FLVRES” motif (FLA**R**PS in the N-SH2, FLV**R**ES in the C-SH2) of each SH2 domain. The N-SH2 mutant (R32->M) retained some ability to rescue cell death, although it was less effective than WT Shp2 (Figures 4B, J). However, the C-SH2 mutant (R138->M) was unable to block cell death in *shp2* morphants (Figures 4B, K). Moreover, the C-SH2 domain alone restored cell survival in morphants (Figures 4B, L). Together, these results show that Shp2 contains an anti-apoptotic function encoded by its SH2 domains, which is PTP- and ERK-independent and inhibits a p53-dependent stress/DNA damage response in the embryonic nervous system, including the neural crest.

Shp2 Has Two Separate Functions During Neural Crest Development

Blocking cell death in *shp2* MO embryos restores some neural crest tissues, but such embryos still have defects in their craniofacial skeletons and in pigment cell number and migration (Figures 1 and 3). We asked whether bypassing Shp2 to activate the Erk pathway, while simultaneously suppressing cell death, could rescue all neural crest phenotypes caused by *shp2* MO injection. To activate Erk, we expressed a gain-of-function mutant of the human RAS guanine nucleotide exchange factor *SOS1* (*SOS1*^{R552G}) found in some NS

patients lacking *PTPN11* (*SHP2*) mutations (Roberts et al., 2007; Tartaglia et al., 2007). Injection of $SOS1^{R552G}$ mRNA at low doses (250 pg/embryo) significantly increased Erk activation in zebrafish embryos at 24 hpf without causing obvious morphological defects (Figure 5A and data not shown). Co-injecting $SOS1^{R552G}$ mRNA and the *shp2* MO did not rescue excessive cell death in MO-injected embryos (compare Figures 5B–D), consistent with the Erk pathway-independent, anti-apoptotic function of Shp2. In contrast, cell death was prevented when *shp2* MO was injected into *p53* mutant embryos (data not shown, but see Figure 5E), but these embryos exhibited a neural crest phenotype similar to LS mRNA injected embryos (compare Figures 1D and 5H). As expected, $SOS1^{R552G}$/*shp2* MO-co-injected embryos showed decreased pigment cells and branchial arch structures (Figure 5I), phenotypes observed in embryos injected with *shp2* MO alone (compare Figures 1 and 5I). Migration of pigment cells to the ventral stripe was restored in these animals (compare arrows in Figures 5G–I), consistent with the Erk-dependency of the migration defect in morphants. Finally, we co-injected $SOS1^{R552G}$ mRNA with the *shp2* MO into *p53* homozygous mutant animals, simultaneously restoring Erk activation and blocking cell death. This combination resulted in normal pigmentation, branchial arches and migration to the ventral stripe in ~70% of injected animals (Figure 5J). Hence, Shp2 is essential for (at least) two independent pathways needed for normal neural crest development: one that requires Shp2 catalytic activity to evoke proper Ras/Erk pathway activation, and another in which PTP activity and Erk activation are dispensable, but the Shp2 SH2 domains are required, to prevent activation of a p53-dependent cell death pathway (see Figure 7D).

Both *SHP2*-Dependent Pathways Are Conserved in Human Neural Crest Cells

We asked whether the above pathways are conserved in human neural crest-derived cell systems. To investigate the ERK-dependent pathway, we used 501mel melanoma cells. Using *SHP2-shRNA#2*, one of the three lentivirus-encoded *shRNAs* that knock down *SHP2* to various extents in neural crest-derived cells (see Figures 6A, 7A and S4), we infected 501mel cells and generated a stable pool with decreased SHP2 levels (Figure 6A). As expected, these cells showed impaired growth factor-induced ERK activation (Figure 6B). Furthermore, expression of neural crest pluripotency markers (*SOX10, FOXD3, EDNRB* and *DCT)* was increased, while expression of *GAPDH* and the differentiation markers *MITF* and *TRPM1* were unchanged (Figure 6C). Treatment of WT 501mel cells and other melanoma cell lines (e.g., Malme3m) with U0126 also increased *SOX10* and *FOXD3* expression (Figure 6D and data not shown). These data suggest that, consistent with our zebrafish findings, loss of SHP2 and the consequent decrease in ERK activation, alter the gene regulatory network in mammalian neural crest cells, promoting the expression of pluripotency markers.

Human neuroblastoma cells typically have an intact p53 pathway and rarely harbor activating mutations in the RAS/RAF/ERK pathway, allowing us to interrogate the PTP- and ERK-independent effects of SHP2. Transduction of *SHP2-shRNAs* into neuroblastoma cell lines reduced SHP2 levels and inhibited ERK activation (Figures 7A, B), with *SHP2-shRNA#3* being the most effective (Figure S4). One line (KELLY) showed significantly increased γ-H2Ax levels, PARP cleavage and TUNEL labeling when SHP2 levels were suppressed (Figures 7A, C and S4B). Expression of WT zebrafish *shp2* in these cells inhibited γ-H2Ax levels and PARP cleavage and promoted survival by ~ 50% (Figures 7B, C and S4B). Notably, zebrafish *shp2* containing the LS mutation (A462T), the double mutant (A462T/R466M), or the C-SH2 domain alone all suppressed cell death (Figures 7B, C and S4B). We conclude that Shp2 contains a novel, evolutionarily conserved, anti-apoptotic function that is independent of PTP activity and ERK-activation, and functions through its N-terminal SH2 domains.

DISCUSSION

Shp2 catalytic activity is required for activation of the Ras/Erk cascade in response to multiple stimuli and for its cell-type and receptor-specific roles in PI3K/Akt activation, Rho family GTPase regulation, and NF-kB and NFAT activation (Feng, 1999; Neel et al., 2009). We have found that Shp2 has an additional, catalytic– and Erk-independent function, and that both pathways are required in zebrafish and human neural crest cells (Figure 7D). Neural crest specification and migration involve the canonical Shp2/Ras/Erk pathway, acting via Foxd3 and Sox10, while the novel, conserved SH2-domain-dependent, PTP-independent function of Shp2 is required to prevent DNA-damage-induced cell death. The absence of both pathways in *shp2* morphants results in marked abnormalities of multiple neural crest tissues, most notably, pigment and facial cartilage cells. These defects can be rescued by simultaneously providing the Ras/Erk pathway requirement with an activated human *SOS1* allele and blocking cell death with *bcl-xl* or mutant *p53*. In contrast, loss of only the PTP-dependent pathway (e.g., in LS mRNA-injected embryos) leads to excess pigment cells and craniofacial dysmorphia, features that resemble LS. Our results provide a conceptual framework for resolving the paradoxical effects of human disease-associated *PTPN11* mutants with increased (NS) and decreased (LS) catalytic activity.

Jopling and colleagues also observed craniofacial and heart defects in *shp2* MO- and LS-injected zebrafish embryos (Jopling et al., 2007). Subsequently, two groups showed that neural crest-specific *Shp2* deletion in mice causes defective specification and migration, resulting in craniofacial, heart and glial defects (Grossmann et al., 2009; Nakamura et al., 2009). Here, we provide insight into the underlying mechanisms downstream of Shp2 that cause these neural crest defects, first by showing that either *shp2* knockdown or expression of LS mutant *shp2* causes inappropriate expression of *foxd3* and *sox10*. These effects are Erk-dependent and not an indirect consequence of defective gastrulation, as they also are evoked by Mek inhibitor treatment post-gastrulation (Figure 2). *SOX10* and *FOXD3* are also inhibited in human melanoma cells transduced with *SHP2-shRNA* or treated with U0126 (Figures 6C, D). High levels of *Sox10* or *FoxD3* in neural crest and embryonic stem cells promote multi-potentiality (Kim et al., 2003; Teng et al., 2008). These findings suggest that suppression of Erk signaling, resulting from Shp2 knockdown or LS mutant expression, promotes the maintenance of pluripotent progenitor cell fate (due to increased Sox10 and possibly Foxd3 levels), which in turn blocks, or at least delays, neural crest differentiation and migration (Figure 7D). Pigment cells are one of the last neural crest lineages to be specified (and migrate along a lateral pathway), so delayed specification would be expected to cause excessive pigmentation (Raible and Eisen, 1996). Consistent with our model, forced expression of *sox10* during neural crest specification causes excess pigment cells (Figure 2C). The delayed migration of neural crest progenitors and pigment cells caused by high levels of Sox10 could be a consequence of delayed specification, or may be due to other, more direct Shp2- and Erk-dependent mechanisms.

The early effects of Shp2 deficiency or LS mRNA injection can be explained by decreased Shp2 catalytic activity and Erk activation. Later, their effects differ dramatically, with Shp2 deficiency leading to neural crest cell death, while LS-injected embryos show increased numbers of many neural crest-derived cell types, including iridophores, melanophores, and sympathetic neurons (Figures 1E and S2). The excess cell death in *shp2* morphants is *p53*-dependent, and can be rescued by WT Shp2, Shp2 mutants with impaired (LS) or absent (R466M) catalytic activity, or even constructs containing only the SH2 domains or even the C-SH2 domain alone (Figures 3 and 4). Thus, the Shp2-mediated anti-apoptotic pathway must be PTP- and Erk-independent. Importantly, this pathway is also conserved in mammalian neural crest-derived (KELLY) cells.

How the Shp2 SH2 domains prevent p53 induction remains to be elucidated. Mutagenesis studies suggest that the C-SH2, most likely in concert with the N-SH2 (Figure 4J), must bind to one or more specific pTyr-proteins at a key time during development. C-SH2 binding could act directly to alter signaling by the pTyr-protein or it could competitively inhibit the binding of other SH2 or PTB domain-containing proteins to the critical pTyr-protein. Notably, the binding sites for the SH2 domains of Shp2, Shp1, Ship-1, Ship2, and Socs3 overlap considerably (Neel et al., 2009). In the absence of Shp2, there could be increased binding of one of more of these proteins to the pTyr-protein in question, which in turn could activate DNA damage-induced apoptosis. Alternatively, the Shp2 C-SH2 domain could bind and regulate a novel pTyr-protein, and the absence of its interaction with Shp2 could result in triggering *p53*-dependent cell death. Future studies of KELLY cells, which require SHP2 for viability, should facilitate the identification of molecules downstream of SHP2 that are required to suppress p53 activation. Indeed, preliminary 'pull-down' experiments using GST-SH2 fusion proteins and *SHP2*-knockdown and control KELLY cell lysates have identified several candidates. Further analysis of these binding partners will be required to elucidate the mechanisms underlying SHP2's role in neural crest cell survival.

Previous studies indicate a role for Shp2 in preventing cell death in other stem/progenitor cell populations. For example, conditional deletion of murine *Ptpn11* in early neuronal cells results in increased cell death (Ke et al., 2007). We also saw increased neuronal cell death in *shp2* morphants, but not LS mutant mRNA-injected embryos. Thus, Shp2 catalytic activity may be dispensable for its anti-apoptotic effects in neurons. Homozygous null mutation of murine *Ptpn11* results in peri-implantation lethality and death of trophoblast stem cells. These cells have reduced Erk activation, decreased Erk phosphorylation of the pro-apoptotic BH3 protein Bim-EL, and Bim-EL stabilization (Yang et al., 2006). Because Bim depletion substantially (but not completely) restores viability to *Ptpn11*-deleted trophoblast stem cells, Shp2 appears to prevent death in part by promoting Erk-dependent Bim degradation. Although these data implicated Bim in cell death, they did not formally demonstrate a requirement for Erk activity or for Shp2 catalytic activity in preventing apoptosis. In any event, the Shp2>Erk>Bim pathway accounts for only half of the observed cell death in *Ptpn11*-deficient trophoblast stem cells (Yang et al., 2006). The partial rescue of cell death in KELLY cells by catalytically inactive zebrafish *shp2* constructs (Figure 7C) raises the possibility that other SHP2-regulated anti-apoptotic pathways also may function in these cells. SV40 large T-immortalized fibroblasts from *Ptpn11* exon $3^{-/-}$ embryos are resistant to cell death in response to DNA-damaging agents and expression of WT, but not catalytically impaired, Shp2 restores DNA damage-induced cell death (Yuan et al., 2003a; Yuan et al., 2003b). Although these data indicate that Shp2 is required for DNA-damaged induced apoptosis in these cells, large T-antigen inactivates p53, and thus blocks the in vivo apoptotic pathway that we have defined.

Our results have important implications for the pathogenesis of human diseases caused by germline *PTPN11* mutations. The combined effects of LS-specific neural crest phenotypes can be explained by impairment of Shp2-mediated Erk activation and retention of Shp2's ability to block apoptosis (Figure 7D). Defective Erk activation, acting via Sox10 (Figure 2C) and possibly FoxD3 (Figures 2 and 6), results in mis-specification of neural crest progenitors, leading to an excess of some tissues (pigment, sympathetic neurons) at the expense of others (cartilage), as well as impaired migration. In *shp2* morphants, these excess cells die, whereas in LS mutant-injected fish, they survive. The resulting effects on neural crest specification, together with defective neural crest cell migration, could account for the LS phenotype. NS mutants, in contrast, should reduce or have no effect on neural crest progenitor numbers (depending on the threshold of Erk activity required), while retaining the ability to prevent neural crest cell death. Indeed, zebrafish embryos injected with mRNA for the NS mutant D61G show gastrulation phenotypes similar to LS-injected embryos, but

display no differences in early neural crest gene expression or pigmentation (Jopling et al., 2007; and our unpublished observations). Furthermore, *shp2* mutants associated with LS and NS don't have additive or synergistic effects on zebrafish gastrulation, providing additional evidence that these mutants act in distinct ways (Jopling et al., 2007).

Finally, our findings provide new insights into SHP2-mediated oncogenesis. Oncogenic *PTPN11* mutations preferentially cause SHP2 to be in an "open" conformation, exposing both the PTP domain and SH2 domains (Mohi and Neel, 2007; Tartaglia et al., 2006). Our results suggest that this "open" molecule may have two separate functions that promote tumor formation: a PTP- and Erk-dependent function to promote cell proliferation and growth, and a PTP- and Erk-independent function that prevents p53-induced cell death.

EXPERIMENTAL PROCEDURES

Molecular Biology

MOs were obtained from Gene Tools, LLC. The ATG-MO was used in Figures 1–3 and S1–2 in this study. The Ex3-MO was used in Figures 4, S1 and S3. Both MOs resulted in identical neural crest phenotypes. The LS mRNA (A462T) was used for all comparative studies. Isolation of zebrafish *shp2* cDNA, site-directed mutagenesis, MO sequences, and working concentrations and optimal injection conditions for MOs and mRNAs are described in Supplemental Experimental Procedures. Probes for *sox10, foxd3, snai1b, tfap2a, puma* and *th* were described previously (Stewart et al., 2006). Real-time Q-PCR primer sequences, *SHP2 shRNA* sequences, lentiviral and retroviral construction, packaging and infection conditions are described in Supplemental Experimental Procedures.

Zebrafish Stocks, Immunohistochemistry and Whole-mount In Situ Hybridization

WT and homozygous $p53^{M214K}$ zebrafish were maintained at 28.5°C by standard methods (Berghmans et al., 2005). Staging was performed by morphological criteria (Kimmel et al., 1995). Whole-mount in situ hybridizations, cartilage staining with Alcian blue and whole-mount immunostainings with anti-HuC mAb 16A11 (Molecular Probes), activated Caspase-3 (BD Biosciences) and γ-H2Ax (a gift of Dr. James Amatruda) were performed as described (Jette et al., 2008; Sidi et al., 2008; Stewart et al., 2006). Embryos injected with control (WT) mRNA or *shp2* mmMO were used for comparison and to adjust for developmental delays caused by injection. Quantification of Acridine orange was carried out as described (Sidi et al., 2008). Statistical analyses were carried out using GraphPad Prism (GraphPad Software Inc). Pigment and sympathetic neuron cell count data were evaluated by Student t-test (2-tailed) for 2 sample comparisons, or ANOVA with Bonferroni post-hoc test for > three samples as appropriate; $p<0.05$ was considered significant.

Zebrafish Biochemical Analyses

Extracts were prepared from 24 and 48 hpf embryos (Liu et al., 2003), and protein concentrations determined by Bradford assay (BioRad). Shp2 and Erk immunoblots were performed on lysates from 24 hpf embryos to correspond with cell death assays. Antibodies are described in Supplemental Experimental Procedures. Optimal concentrations of the Mek1/2 inhibitor U0126 (Cell Signaling) were determined by treating embryos with doses from 50μM to 200μM, analyzing morphological phenotypes and carrying out anti-pErk immunoblots (Figure S3A). Embryos were treated with U0126 or DMSO continuously from the tail bud stage, and lysates prepared at 24hpf. Maximal Erk inhibition was observed at 100–150μM.

Mammalian Cell Culture

The human melanoma cell lines Malme3M (ATCC) and 501mel (Dr Ruth Halaban, Yale University, CT) were maintained in Ham's F10 media supplemented with 10% FBS. The 501mel/shLUC and 501mel/shSHP2 stable cell pools were generated by lentiviral transduction followed by puromycin (1μg/mL) selection. The neuroblastoma cell lines KELLY, SH-SY-5Y and BE(2)M17 were cultured in RPMI-1640 medium containing L-glutamine and 10% fetal bovine serum (Sigma-Aldrich). Apoptosis assays are described in Supplemental Experimental Procedures.

Supplementary Material

Refer to Web version on PubMed Central for supplementary material.

Acknowledgments

We thank P. Henion, J. Amatruda, R. Halaban, R. George and C. Levi for reagents, T. Buyal, R. Solovyev and Y. Ahn for technical assistance, K. Kotredes, J. Kanki and B. Baker for zebrafish maintenance, and C. Jette and members of the Look and Neel labs for helpful discussions. This work was supported by grants R01 HL083271 and R37 CA49152 (B.G.N) and R01 CA104605 (A.T.L.). R.A.S is supported by NIH/NINDS award R00 NS058608. S.Z. is supported by a fellowship from Friends for Life, DFCI. T.S. is supported by Children's Leukemia Research Association research grant. M.K. is supported by NIH/NHLBI grant R00 HL088514.

References

Allard JD, Chang HC, Herbst R, McNeill H, Simon MA. The SH2-containing tyrosine phosphatase corkscrew is required during signaling by sevenless. Ras1 and Raf. Development 1996;122:1137–1146.

Araki T, Mohi MG, Ismat FA, Bronson RT, Williams IR, Kutok JL, Yang W, Pao LI, Gilliland DG, Epstein JA, et al. Mouse model of Noonan syndrome reveals celltype- and gene dosage-dependent effects of Ptpn11 mutation. Nat. Med 2004;10:849–857. [PubMed: 15273746]

Arduini BL, Bosse KM, Henion PD. Genetic ablation of neural crest cell diversification. Development 2009;136:1987–1994. [PubMed: 19439494]

Bader-Meunier B, Tchernia G, Mielot F, Fontaine JL, Thomas C, Lyonnet S, Lavergne JM, Dommergues JP. Occurrence of myeloproliferative disorder in patients with Noonan syndrome. J. Pediatr 1997;130:885–889. [PubMed: 9202609]

Barford D, Neel BG. Revealing mechanisms for SH2 domain mediated regulation of the protein tyrosine phosphatase SHP-2. Structure 1998;6:249–254. [PubMed: 9551546]

Berghmans S, Murphey RD, Wienholds E, Neuberg D, Kutok JL, Fletcher CD, Morris JP, Liu TX, Schulte-Merker S, Kanki JP, et al. tp53 mutant zebrafish develop malignant peripheral nerve sheath tumors. Proc. Natl. Acad. Sci. U S A 2005;102:407–412. [PubMed: 15630097]

Digilio MC, Sarkozy A, de Zorzi A, Pacileo G, Limongelli G, Mingarelli R, Calabro R, Marino B, Dallapiccola B. LEOPARD syndrome: clinical diagnosis in the first year of life. Am. J. Med. Genet. A 2006;140:740–746. [PubMed: 16523510]

Dutton KA, Pauliny A, Lopes SS, Elworthy S, Carney TJ, Rauch J, Geisler R, Haffter P, Kelsh RN. Zebrafish colourless encodes sox10 and specifies non-ectomesenchymal neural crest fates. Development 2001;128:4113–4125. [PubMed: 11684650]

Feng GS. Shp-2 tyrosine phosphatase: signaling one cell or many. Exp. Cell. Res 1999;253:47–54. [PubMed: 10579910]

Fragale A, Tartaglia M, Wu J, Gelb BD. Noonan syndrome-associated SHP2/PTPN11 mutants cause EGF-dependent prolonged GAB1 binding and sustained ERK2/MAPK1 activation. Hum. Mutat 2004;23:267–277. [PubMed: 14974085]

Grossmann KS, Wende H, Paul FE, Cheret C, Garratt AN, Zurborg S, Feinberg K, Besser D, Schulz H, Peles E, et al. The tyrosine phosphatase Shp2 (PTPN11) directs Neuregulin-1/ErbB signaling throughout Schwann cell development. Proc. Natl. Acad. Sci. U S A 2009;106:16704–16709. [PubMed: 19805360]

Hanna N, Montagner A, Lee WH, Miteva M, Vidal M, Vidaud M, Parfait B, Raynal P. Reduced phosphatase activity of SHP-2 in LEOPARD syndrome: consequences for PI3K binding on Gab1. FEBS Lett 2006;580:2477–2482. [PubMed: 16638574]

Hof P, Pluskey S, Dhe-Paganon S, Eck MJ, Shoelson SE. Crystal structure of the tyrosine phosphatase SHP-2. Cell 1998;92:441–450. [PubMed: 9491886]

Jette CA, Flanagan AM, Ryan J, Pyati UJ, Carbonneau S, Stewart RA, Langenau DM, Look AT, Letai A. BIM and other BCL-2 family proteins exhibit cross-species conservation of function between zebrafish and mammals. Cell Death Differ 2008;15:1063–1072. [PubMed: 18404156]

Jopling C, van Geemen D, den Hertog J. Shp2 knockdown and Noonan/LEOPARD mutant Shp2-induced gastrulation defects. PLoS Genet 2007;3:e225. [PubMed: 18159945]

Ke Y, Zhang EE, Hagihara K, Wu D, Pang Y, Klein R, Curran T, Ranscht B, Feng GS. Deletion of Shp2 in the brain leads to defective proliferation and differentiation in neural stem cells and early postnatal lethality. Mol. Cell. Biol 2007;27:6706–6717. [PubMed: 17646384]

Keilhack H, David FS, McGregor M, Cantley LC, Neel BG. Diverse biochemical properties of Shp2 mutants. Implications for disease phenotypes. J. Biol. Chem 2005;280:30984–30993. [PubMed: 15987685]

Kelsh RN, Raible DW. Specification of zebrafish neural crest. Results Probl. Cell. Differ 2002;40:216–236. [PubMed: 12353478]

Kim J, Lo L, Dormand E, Anderson DJ. SOX10 maintains multipotency and inhibits neuronal differentiation of neural crest stem cells. Neuron 2003;38:17–31. [PubMed: 12691661]

Kimmel CB, Ballard WW, Kimmel SR, Ullmann B, Schilling TF. Stages of embryonic development of the zebrafish. Dev. Dyn 1995;203:253–310. [PubMed: 8589427]

Kontaridis MI, Swanson KD, David FS, Barford D, Neel BG. PTPN11 (Shp2) mutations in LEOPARD syndrome have dominant negative, not activating, effects. J. Biol. Chem 2006;281:6785–6792. [PubMed: 16377799]

Liu TX, Howlett NG, Deng M, Langenau DM, Hsu K, Rhodes J, Kanki JP, D'Andrea AD, Look AT. Knockdown of zebrafish Fancd2 causes developmental abnormalities via p53-dependent apoptosis. Dev. Cell 2003;5:903–914. [PubMed: 14667412]

McKeown SJ, Lee VM, Bronner-Fraser M, Newgreen DF, Farlie PG. Sox10 overexpression induces neural crest-like cells from all dorsoventral levels of the neural tube but inhibits differentiation. Dev. Dyn 2005;233:430–444. [PubMed: 15768395]

Merks JH, Caron HN, Hennekam RC. High incidence of malformation syndromes in a series of 1,073 children with cancer. Am. J. Med. Genet. A 2005;134A:132–143. [PubMed: 15712196]

Mohi MG, Neel BG. The role of Shp2 (PTPN11) in cancer. Curr. Opin. Genet. Dev 2007;17:23–30. [PubMed: 17227708]

Nakamura T, Gulick J, Colbert MC, Robbins J. Protein tyrosine phosphatase activity in the neural crest is essential for normal heart and skull development. Proc. Natl. Acad. Sci. U S A 2009;106:11270–11275. [PubMed: 19541608]

Neel, BG.; Gu, H.; Pao, L. SH2-Domain-Containing Protein-Tyrosine Phosphatases In Handbook of Cell Signaling, D.E. Bradshaw, RA., editor. Academic Press; 2009. p. 707-729.

Niihori T, Aoki Y, Ohashi H, Kurosawa K, Kondoh T, Ishikiriyama S, Kawame H, Kamasaki H, Yamanaka T, Takada F, et al. Functional analysis of PTPN11/SHP-2 mutants identified in Noonan syndrome and childhood leukemia. J. Hum. Genet 2005;50:192–202. [PubMed: 15834506]

O'Reilly AM, Neel BG. Structural determinants of SHP-2 function and specificity in Xenopus mesoderm induction. Mol. Cell. Biol 1998;18:161–177. [PubMed: 9418864]

Ogata T, Yoshida R. PTPN11 mutations and genotype-phenotype correlations in Noonan and LEOPARD syndromes. Pediatr. Endocrinol. Rev 2005;2:669–674. [PubMed: 16208280]

Pandit B, Sarkozy A, Pennacchio LA, Carta C, Oishi K, Martinelli S, Pogna EA, Schackwitz W, Ustaszewska A, Landstrom A, et al. Gain-of-function RAF1 mutations cause Noonan and LEOPARD syndromes with hypertrophic cardiomyopathy. Nat. Genet 2007;39:1007–1012. [PubMed: 17603483]

Perkins LA, Larsen I, Perrimon N. corkscrew encodes a putative protein tyrosine phosphatase that functions to transduce the terminal signal from the receptor tyrosine kinase torso. Cell 1992;70:225–236. [PubMed: 1638629]

Raible DW, Eisen JS. Regulative interactions in zebrafish neural crest. Development 1996;122:501–507. [PubMed: 8625801]

Razzaque MA, Nishizawa T, Komoike Y, Yagi H, Furutani M, Amo R, Kamisago M, Momma K, Katayama H, Nakagawa M, et al. Germline gain-of-function mutations in RAF1 cause Noonan syndrome. Nat. Genet 2007;39:1013–1017. [PubMed: 17603482]

Roberts AE, Araki T, Swanson KD, Montgomery KT, Schiripo TA, Joshi VA, Li L, Yassin Y, Tamburino AM, Neel BG, et al. Germline gain-of-function mutations in SOS1 cause Noonan syndrome. Nat. Gen.et 2007;39:70–74.

Robu ME, Larson JD, Nasevicius A, Beiraghi S, Brenner C, Farber SA, Ekker SC. p53 activation by knockdown technologies. PLoS Genet 2007;3:e78. [PubMed: 17530925]

Saxton TM, Henkemeyer M, Gasca S, Shen R, Rossi DJ, Shalaby F, Feng GS, Pawson T. Abnormal mesoderm patterning in mouse embryos mutant for the SH2 tyrosine phosphatase Shp-2. EMBO J 1997;16:2352–2364. [PubMed: 9171349]

Schubbert S, Zenker M, Rowe SL, Boll S, Klein C, Bollag G, van der Burgt I, Musante L, Kalscheuer V, Wehner LE, et al. Germline KRAS mutations cause Noonan syndrome. Nat. Genet 2006;38:331–336. [PubMed: 16474405]

Shi ZQ, Yu DH, Park M, Marshall M, Feng GS. Molecular mechanism for the Shp-2 tyrosine phosphatase function in promoting growth factor stimulation of Erk activity. Mol. Cell. Biol 2000;20:1526–1536. [PubMed: 10669730]

Sidi S, Sanda T, Kennedy RD, Hagen AT, Jette CA, Hoffmans R, Pascual J, Imamura S, Kishi S, Amatruda JF, et al. Chk1 suppresses a caspase-2 apoptotic response to DNA damage that bypasses p53, Bcl-2,and caspase-3. Cell 2008;133:864–877. [PubMed: 18510930]

Stewart RA, Arduini BL, Berghmans S, George RE, Kanki JP, Henion PD, Look AT. Zebrafish foxd3 is selectively required for neural crest specification, migration and survival. Dev. Biol 2006;292:174–188. [PubMed: 16499899]

Tang TL, Freeman RM Jr, O'Reilly AM, Neel BG, Sokol SY. The SH2-containing protein-tyrosine phosphatase SH-PTP2 is required upstream of MAP kinase for early Xenopus development. Cell 1995;80:473–483. [PubMed: 7859288]

Tartaglia M, Gelb BD. Noonan syndrome and related disorders: genetics and pathogenesis. Annu. Rev. Genomics Hum. Genet 2005;6:45–68. [PubMed: 16124853]

Tartaglia M, Martinelli S, Stella L, Bocchinfuso G, Flex E, Cordeddu V, Zampino G, Burgt I, Palleschi A, Petrucci TC, et al. Diversity and functional consequences of germline and somatic PTPN11 mutations in human disease. Am. J. Hum. Genet 2006;78:279–290. [PubMed: 16358218]

Tartaglia M, Pennacchio LA, Zhao C, Yadav KK, Fodale V, Sarkozy A, Pandit B, Oishi K, Martinelli S, Schackwitz W, et al. Gain-of-function SOS1 mutations cause a distinctive form of Noonan syndrome. Nat. Genet 2007;39:75–79. [PubMed: 17143282]

Teng L, Mundell NA, Frist AY, Wang Q, Labosky PA. Requirement for Foxd3 in the maintenance of neural crest progenitors. Development 2008;135:1615–1624. [PubMed: 18367558]

Ucar C, Calyskan U, Martini S, Heinritz W. Acute myelomonocytic leukemia in a boy with LEOPARD syndrome (PTPN11 gene mutation positive). J. Pediatr. Hematol. Oncol 2006;28:123–125. [PubMed: 16679933]

Yang W, Klaman LD, Chen B, Araki T, Harada H, Thomas SM, George EL, Neel BG. An Shp2/SFK/Ras/Erk signaling pathway controls trophoblast stem cell survival. Dev Cell 2006;10:317–327. [PubMed: 16516835]

Yuan L, Yu WM, Qu CK. DNA damage-induced G2/M checkpoint in SV40 large T antigen-immortalized embryonic fibroblast cells requires SHP-2 tyrosine phosphatase. J. Biol. Chem 2003a;278:42812–42820. [PubMed: 12937170]

Yuan L, Yu WM, Yuan Z, Haudenschild CC, Qu CK. Role of SHP-2 tyrosine phosphatase in the DNA damage-induced cell death response. J. Biol. Chem 2003b;278:15208–15216. [PubMed: 12594211]

Zhang SQ, Yang W, Kontaridis MI, Bivona TG, Wen G, Araki T, Luo J, Thompson JA, Schraven BL, Philips MR, et al. Shp2 regulates SRC family kinase activity and Ras/Erk activation by controlling Csk recruitment. Mol. Cell 2004;13:341–355. [PubMed: 14967142]

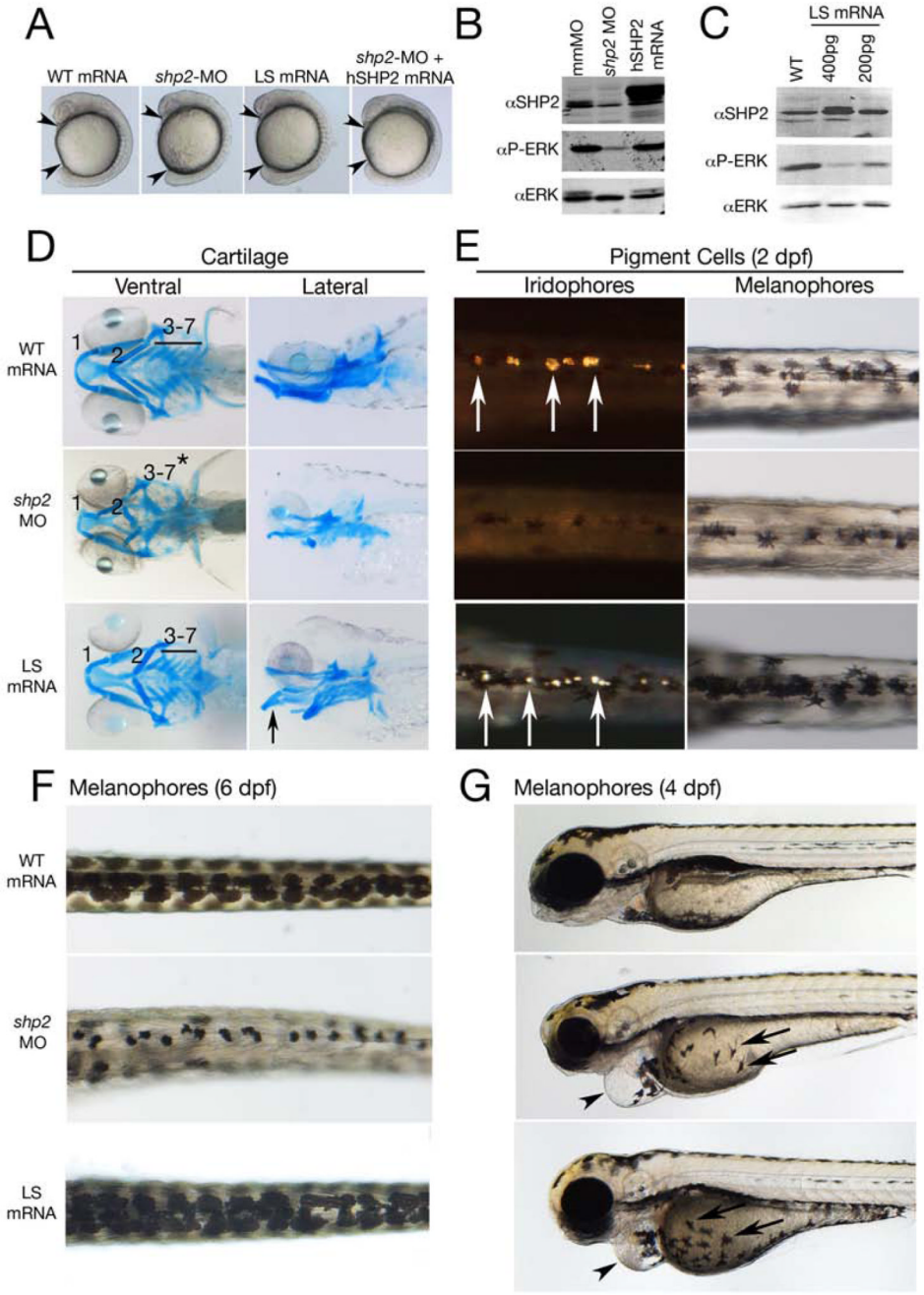

Figure 1. Effects of LEOPARD syndrome mutants are not equivalent to *shp2* deficiency

(A) Lateral views of 18-somite stage embryos injected with the indicated mRNAs or MOs. Arrowheads indicate distance between the head and tail. (B) Immunoblot showing lysates from embryos injected with the *shp2* MO, compared with control (mmMO) or WT human *PTPN11 (hSHP2) mRNA*. Total Erk is indicated as a loading control. (C) Immunoblot showing dose-dependent dominant negative effects on pErk levels in embryos injected with LS^{A462T} mRNA compared to un-injected controls (WT). (D) Alcian blue stains of 6 dpf embryos injected with indicated mRNAs or *shp2* MO. Left panels: ventral view; right panels: lateral view. (E) Dorsal views of 2 dpf embryos, in dark (left) and bright (right) field, showing loss of iridophores (white arrows) and melanophores in *shp2* MO-injected

embryos. LS mRNA injection increases pigment cell numbers. (F) Dorsal views of melanophores at 6 dpf, showing pigment cells in WT mRNA-, MO-, and LS mRNA-injected embryos. (G) Lateral views of 4 dpf embryos. Note delayed migration of melanophores to the yolk in MO- and LS mRNA-injected embryos (black arrows), cardiac edema (arrowheads) and jaw defects. See Figure S1 for additional quantification and data.

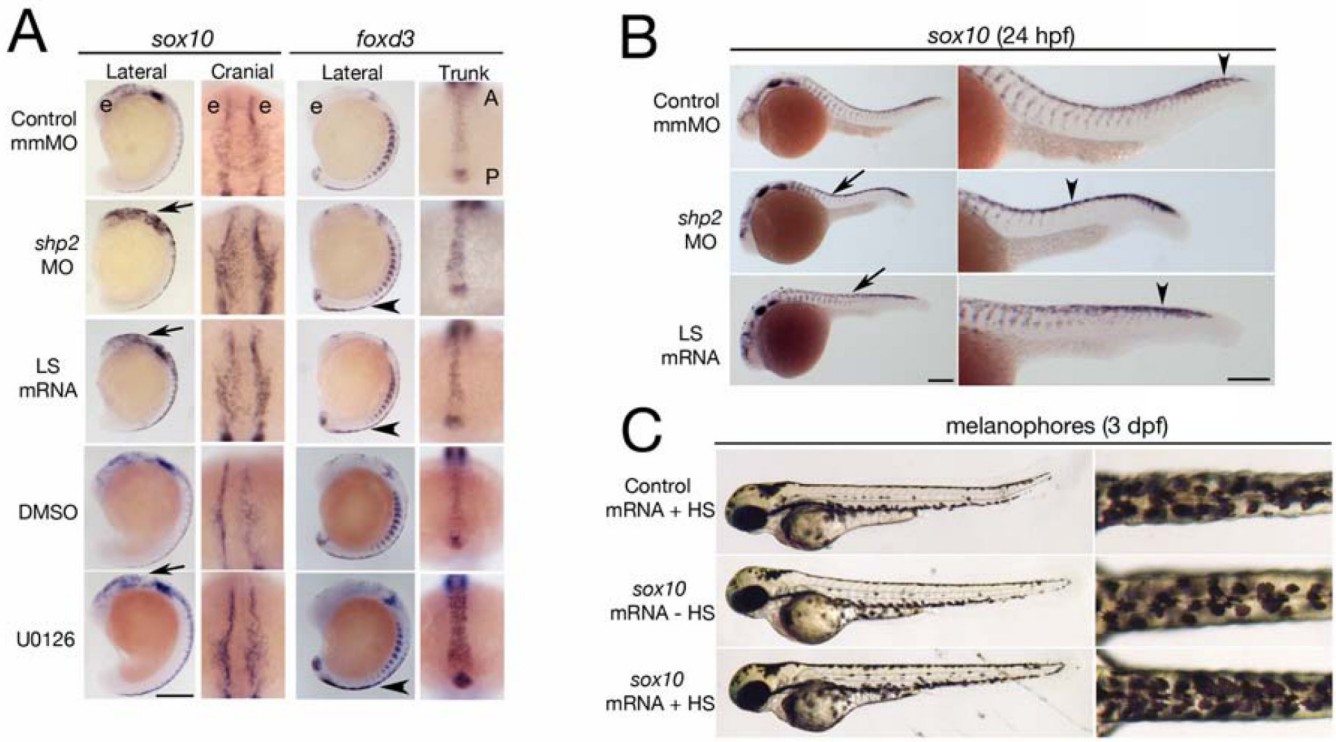

Figure 2. Phosphatase- and Erk-dependent role of Shp2 in neural crest specification and migration

(A) Indicated views of in situ hybridizations with *sox10* and *foxd3* probes from control, MO-, LS mRNA-injected, DMSO and U0126 treated embryos (16–18 somites). The head is to the top in all views. Note increased *sox10* expression in the cranial neural crest in MO- and LS mRNA-injected embryos (arrows). Cranial views of the same region indicated by the arrow show delayed neural crest migration. At the same stage, *foxd3* expression is elevated in trunk neural crest (arrowheads indicate region of higher magnification views). WT embryos treated with U0126 (150 μM) at the tailbud stage show elevated *sox10* and *foxd3* expression and delayed migration in cranial and trunk neural crest. (B) Lateral views of 26 somite embryos showing increased *sox10* expression in MO- and LS mRNA-injected embryos in the head and along the dorsal midline (arrows). Trunk neural crest migration, as indicated by the most posterior migrating cells (arrowheads), also is delayed. Right panels show higher magnifications. (C) Lateral (left) and dorsal (right) views of WT embryos injected with control (*gfp*) or heat shock-inducible *sox10* mRNA. A 2 hr heat shock at the 16- to 18-somite stage causes increased pigmentation in *sox10* mRNA-injected embryos at 3 dpf; see Figure S2 for quantification and data. Scale bars are 200μ, position of the eye (e) and the anterior-posterior (A–P) position in the trunk views is indicated.

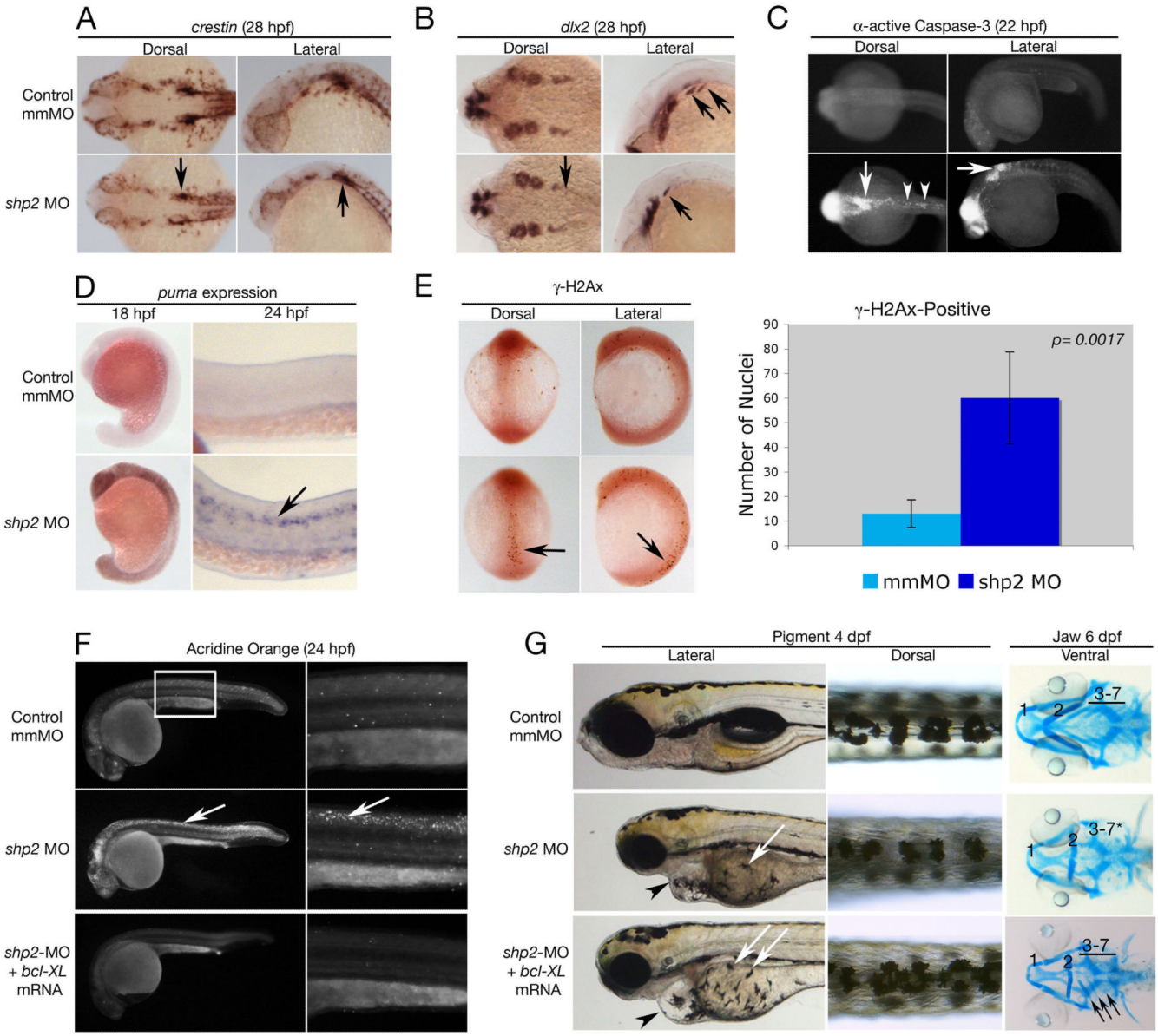

Figure 3. Loss of*shp2*causes cell death in neural tissue

(A, B) Embryos (28 hpf) stained for the pan-neural crest marker *crestin* (A), or *dlx2* (B). *shp2* MO causes a severe loss of *crestin*- and *dlx2*-positive neural crest cells posterior to the otic placode (black arrows in A and B). (C) Views of 22 hpf embryos stained for α-activated-Caspase 3. Lack of *shp2* causes apoptosis in the head and cells adjacent to the otic placode (arrows), extending down the dorsal region of the trunk (arrowheads). (D) Lateral views show increased *puma* expression in morphants at 18 hpf, particularly in the brain (left panels), which by 24 hpf becomes restricted to the neural tube (arrow in right panel). (E) Depletion of *shp2* causes an increase in γ-H2Ax-positive nuclei in 12-somite stage embryos along the dorsal midline (quantified at right). (F) Lateral views (30x) of Acridine orange-stained embryos (24hpf); right panels are higher magnification views (80x) of the trunk region (boxed). Cell death in the spinal cord (arrows) and brain is rescued by co-expressing zebrafish *bcl-xl* mRNA with *shp2* MO. (G) Lateral (left) and Dorsal (right) views of 4 dpf embryos, showing that co-expression of zebrafish *bcl-xL* mRNA restores pigment cell

numbers, but not their migration to the ventral stripe (white arrows). Right panels: Ventral views of 6 dpf embryos stained with Alcian blue, showing rescue of some cartilage elements (arrows).

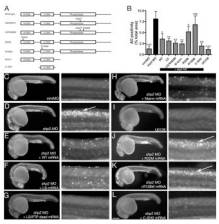

Figure 4. Anti-apoptotic function of Shp2 is mediated by its SH2 domains

(A) Schematic of Shp2 mutants (also see Figure S1A). (B) Acridine orange uptake in the dorsal neural tube of zebrafish embryos injected with the indicated mRNAs. (C–L) Paired lateral views of 24 hpf embryos stained with Acridine orange; for each pair, the right panel shows a higher magnification image. (C) Control MO. (D) *shp2* Ex3-MO causes cell death in the developing brain and spinal cord (arrow). Co-expression of WT *shp2* (E), an LS mutant (A462T) (F), an A462T/R466M double mutant (G), or a truncation mutant that removes the PTP domain and C-terminus (H), also blocks cell death. (I) WT embryos treated U0126 do not mimic the morphant cell death phenotype. (J, K) Co-expression of *shp2* mRNA with an N-SH2 point mutation (J) partially blocks cell death in the trunk; C-SH2 point mutations (K) fail to rescue. Co-expression of the C-SH2 domain alone rescues MO-induced cell death (L). Scale bars represent 200μ. See Figures S1A and S3 for supporting data.

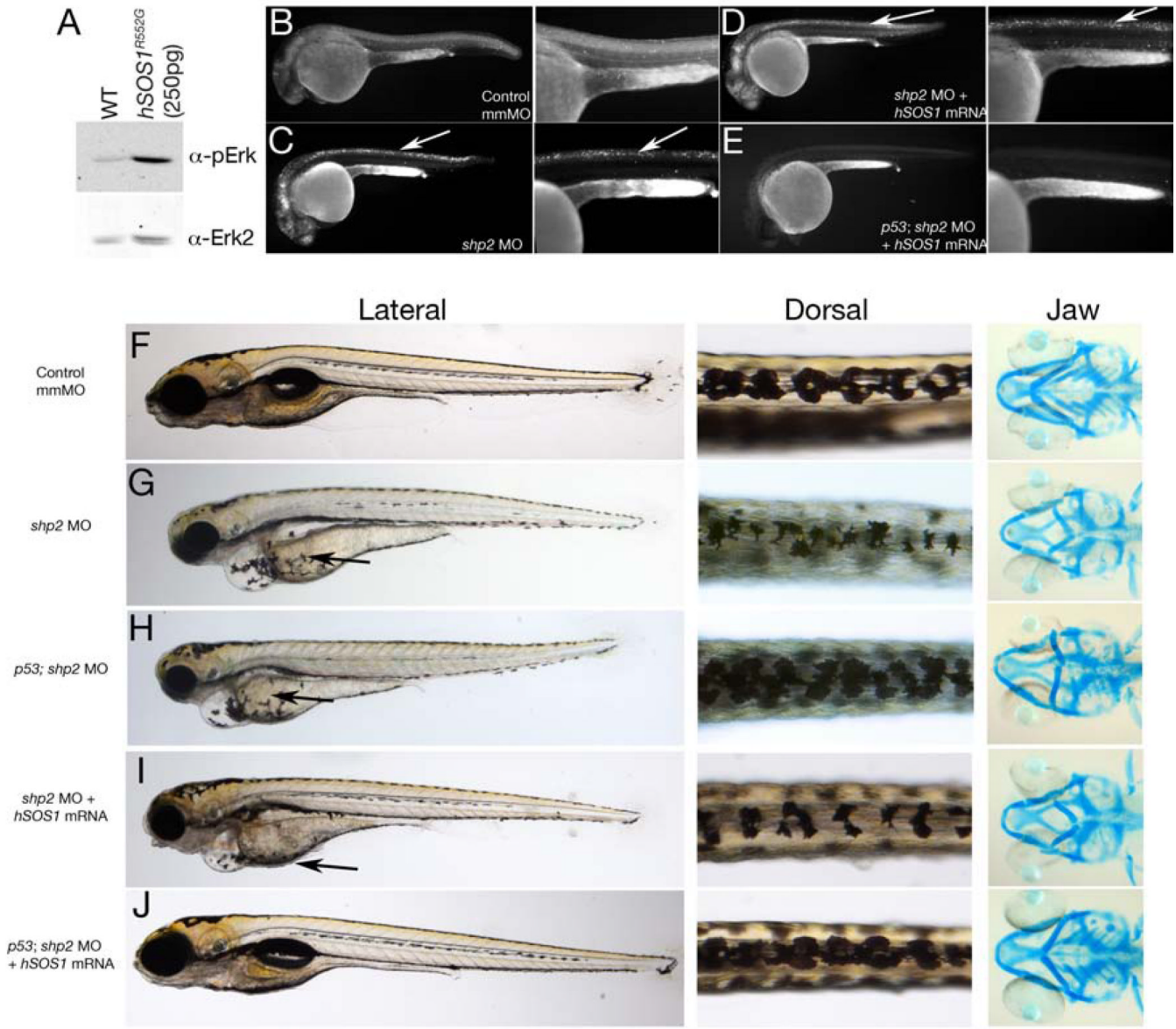

Figure 5. Restoring both Shp2-dependent pathways in*shp2* MO embryos rescues neural crest phenotypes

(A) Immunoblot showing effect of *hSOS1*^{R552G} mRNA on Erk activation. (B–E) Lateral views of Acridine orange labeling in 24 hpf embryos. Cell death caused by *shp2* MO (arrows in C) is not rescued by co-expression with *hSOS1*^{R552G} mRNA (arrows in D) in WT embryos, but is rescued in *p53* mutant embryos (E). (F–J) Lateral (left) and dorsal (middle) views of live 5 dpf embryos and ventral views (right) of 6 dpf embryos stained with Alcian blue. (G) Injection of *shp2* MO causes severe jaw, heart and pigmentation defects and delayed cell migration (arrow). (H) Injection of the *shp2* MO into *p53* mutant embryos partially rescues the jaw defects, but restores pigment cell numbers, although migration is still delayed (arrows in G, H). (I) Migration of pigment cells to the ventral stripe is rescued in *shp2* MO embryos co-injected with *hSOS1*^{R552G} mRNA (arrow), but pigment cell numbers are still reduced, particularly along the dorsal stripe (arrowheads), and embryos have smaller heads, heart edema and severe craniofacial defects. (J) Co-injection of *hSOS1*^{R552G} mRNA into *p53* mutant embryos completely rescues neural crest phenotypes.

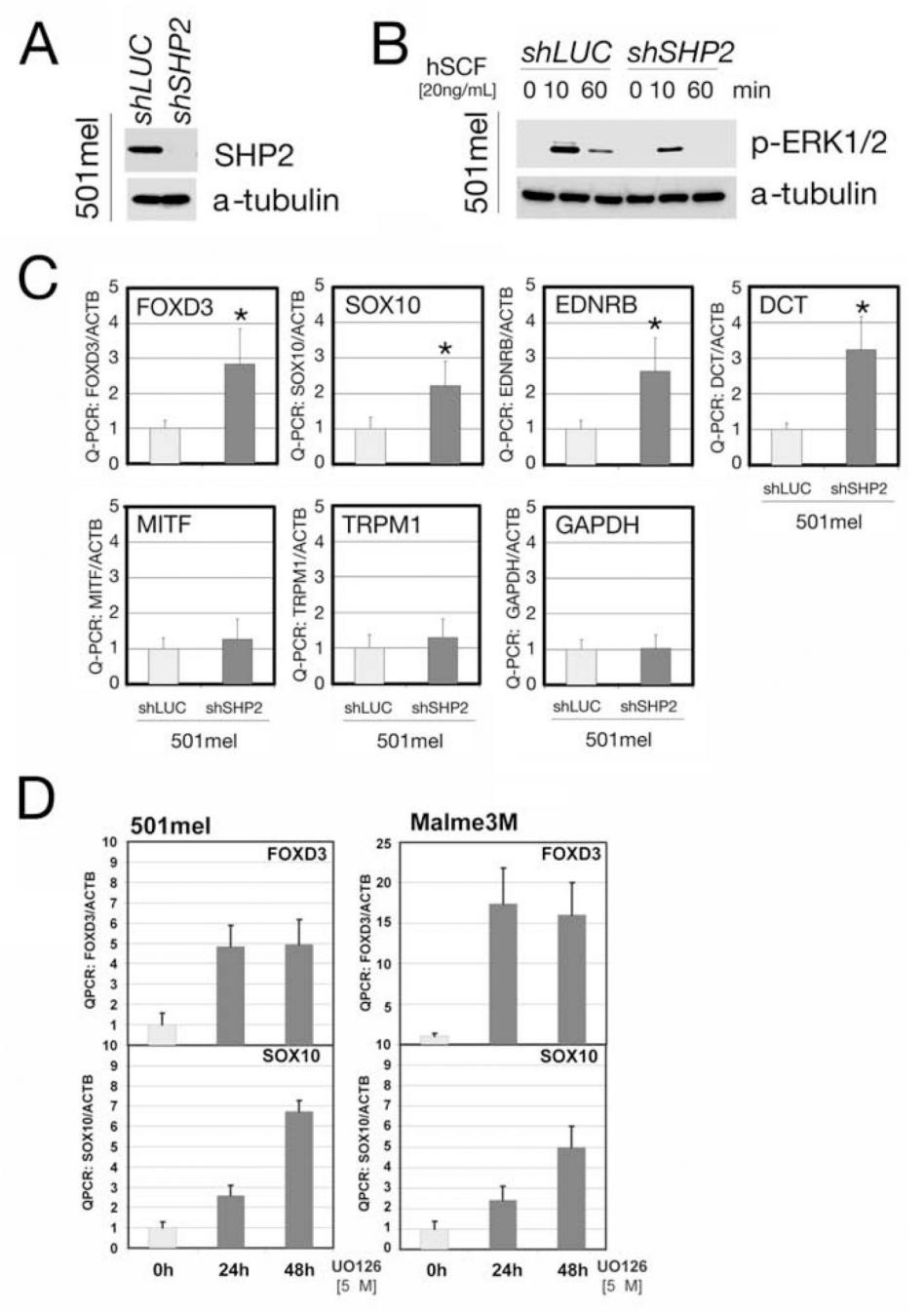

Figure 6. SHP2 regulates transcription factors in human neural crest-derived cells

(A) Immunoblot of lysates from 501mel cells stably expressing *SHP2-shRNA*. (B) Erk activation in 501mel cells transduced with *SHP2-shRNA#2* or shLUC lentivirus at the indicated times after stem cell factor stimulation (hSCF). (C) Levels of neural crest and melanocyte transcription factors in *shRNA*-transduced 501mel cells, determined by Q-PCR. SHP2 deficiency increases transcription of early progenitor (*SOX10, FOXD3, DCT* and *EDNRB)*, but not differentiation (*MITF*, *TRPM1)* markers. *GAPDH* is included as a control and all levels are expressed as ratios relative to β-actin (internal control). Asterisk: $p < 0.05$ by Students t-test. (D) Levels of neural crest and melanocyte markers in 501mel and

Melme3M cells after U0126 treatment, showing that the negative regulation of *SOX10* and *FOXD3* is ERK-dependent.

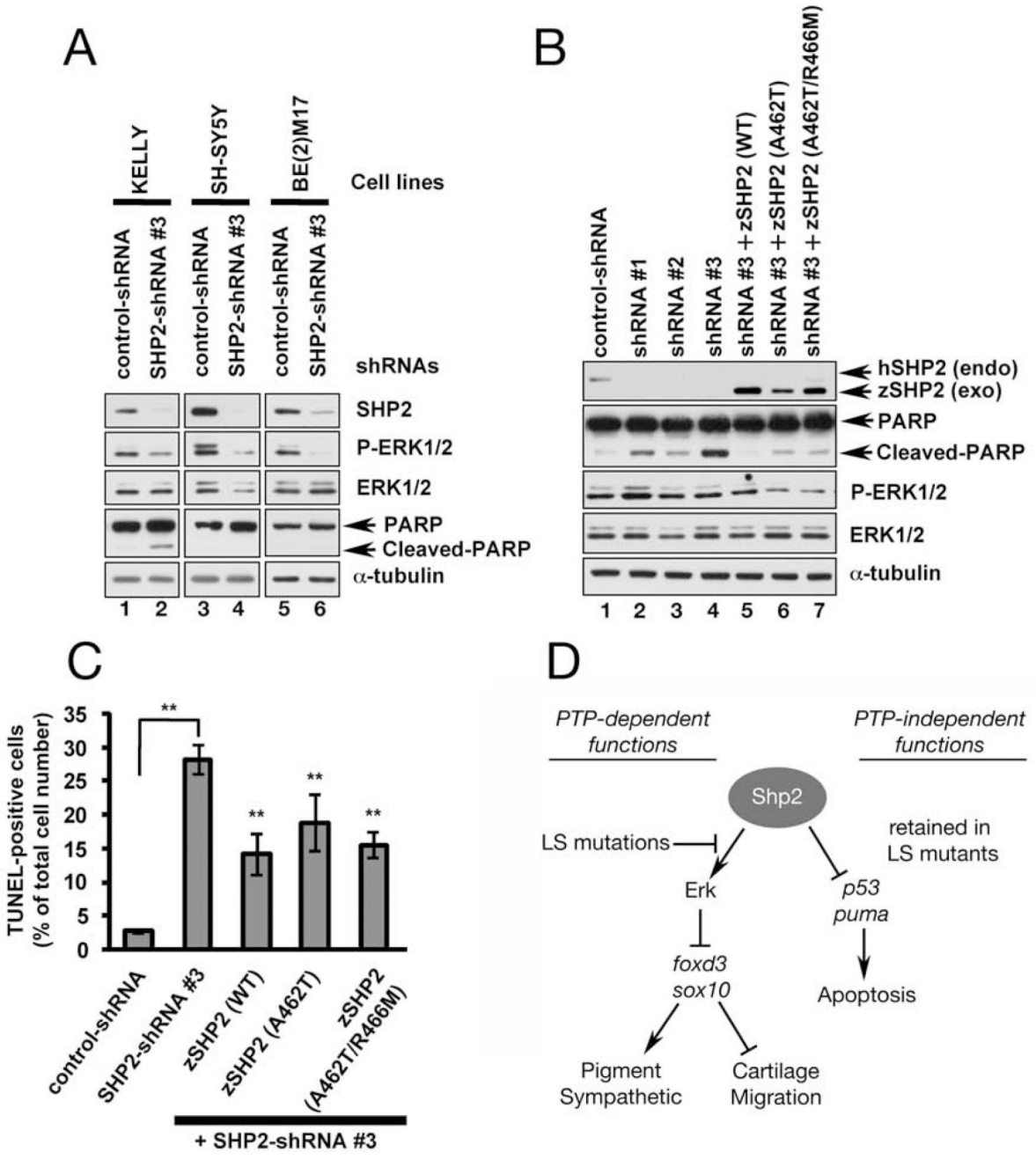

Figure 7. PTP- and ERK-independent function of SHP2 is conserved in neuroblastoma cells

(A) Immunoblot of lysates from neuroblastoma cell lines transduced with control *shRNA* or *SHP2-shRNA#3*. SHP2 and p-ERK1/2 levels are reduced by shRNA#3 in all cell lines (lanes 2, 4, 6), but only KELLY cells exhibit increased PARP cleavage (lane 2). (B) KELLY cells transduced with *SHP2-shRNAs* (#1–3) have decreased SHP2 and ERK1/2 levels and increased PARP cleavage (compare lane 1 to lanes 2–4). PARP cleavage caused by *shRNA#3* is rescued by co-transduction of wild-type zebrafish *zshp2*, PTP-impaired (A462T) or PTP-dead (A462T/R466M) *zshp2*. Exogenous WT *zshp2* partially rescues p-ERK1/2 levels (while LS or LS/PTP-dead *zshp2* have mild dominant negative effects). (C) *shRNA#3* induces cell death in ~ 30% of the infected KELLY cells (TUNEL stain). Co-transduction

with zebrafish constructs reduces the cell death caused by shRNA#3. **p <0.001. (D) Model showing phosphatase-dependent and –independent functions of Shp2 during neural crest development. See text for details and Figure S4 for supporting data.